Thermochimica Acta, 6 (1973) 67–83

THE EFFECTS OF SAMPLE SIZE AND HEATING RATE ON THE KINETICS OF THE THERMAL DECOMPOSITION OF $CaCO_3$

P. K. GALLAGHER AND D. W. JOHNSON, Jr.
Bell Telephone Laboratories, Murray Hill, N.J. 07974 (U. S. A.)
(Received 1 September 1972)

ABSTRACT

Isothermal and dynamic methods were used to study the rate of weight loss of $CaCO_3$. Sample sizes were controlled in the range of 1–32 mg. The contracting area rate law proved universally applicable. A pronounced dependence of the activation enthalpy, pre-exponential term, and rate constant upon sample weight and heating rate was observed. This dependence is discussed primarily in terms of the effects of self-cooling and sample geometry. The concept of a unique activation energy is questioned.

INTRODUCTION

The kinetics of the thermal decomposition of solid state materials is a highly complex and frequently controversial subject. The practical importance of the subject, however, has lead to a very extensive effort to understand the mechanisms which control such reactions. Two of the major experimental difficulties encountered are the effect of the enthalpy of the reaction upon the sample temperature and the control of the atmosphere for those reactions which involve a gaseous reactant or product. These experimental uncertainties are inherent in both the isothermal and dynamic techniques.

There are at least two recognized approaches which should minimize these problems. First, use as small a sample as will provide the necessary experimental sensitivity. Provided that it is in good contact with the heat sink, generally the sample holder, it will allow for better thermal exchange. Since the quantity of gas which is involved is less and its diffusion path shorter, the build up of product gas or depletion of the reactant gas will be minimized. Secondly, work in the region where the reaction is relatively slow. This also releases or consumes less gas and heat per unit of time and thereby reduces these complications. In the isothermal case this can be achieved by working in the lower portion of the practical temperature range and for the dynamic technique by using a relatively slow rate of heating.

It is the purpose of this paper to carefully determine the effects of sample size and heating rate upon a well-defined thermal decomposition in order to determine the validity or effectiveness of these approaches. The decomposition of calcium carbonate has been frequently studied[1] and shown to be reversible and straight

forward. However, there have been no extensive studies of the dependence upon sample size and heating rate. The relatively large weight loss associated with the evolution of carbon dioxide also provides an experimentally convenient and accurate technique for following the course of the decomposition.

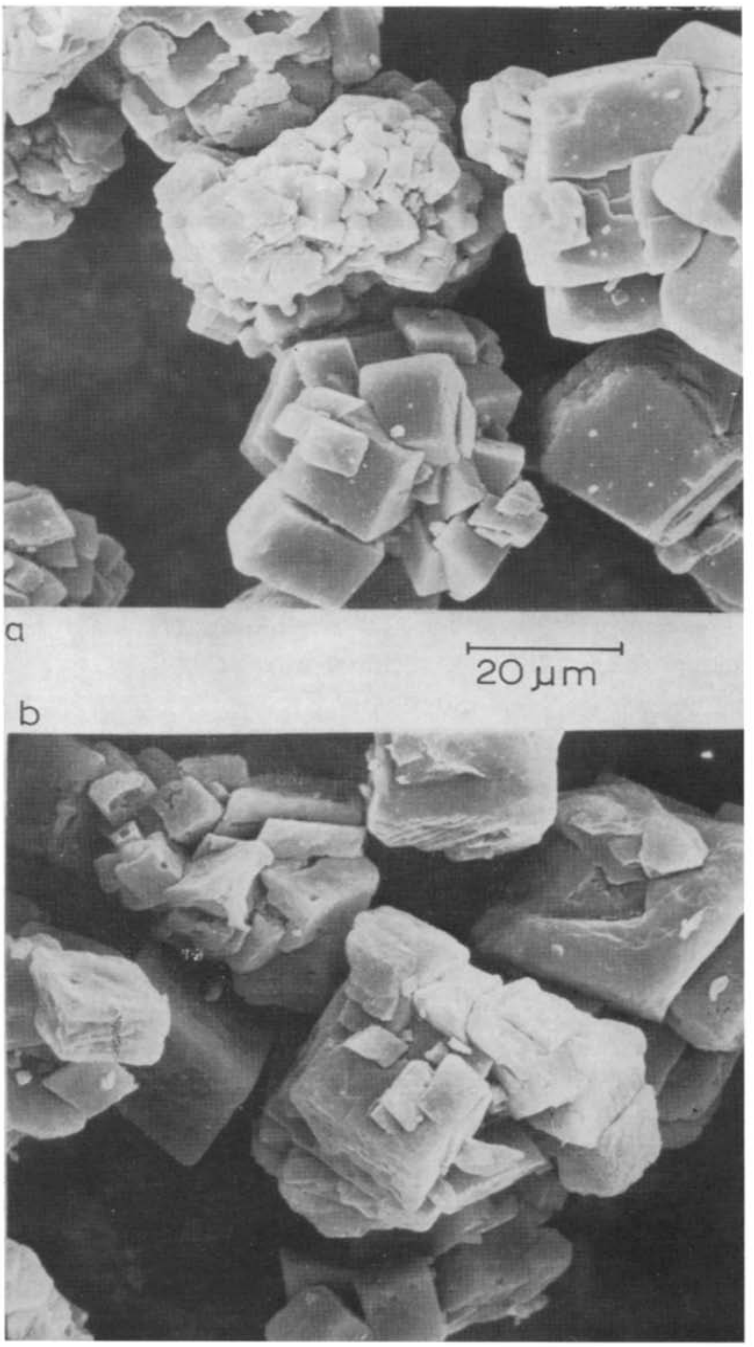

Fig. 1. Scanning electron micrographs of calcium carbonate: a, before decomposition, and b, after decomposition.

EXPERIMENTAL PROCEDURES AND RESULTS

The calcium carbonate was reagent grade from the J. T. Baker Co. It was seived and the fraction from 20–44 μm was selected for study. The surface area was measured by nitrogen absorption (BET technique) and found to be 1.4 $m^2 g^{-1}$. Assuming spherical geometry and a density of 2.71 $g cm^{-3}$ this indicates an average particle size of about 1.6 μm and suggests that many of the seived particles were actually agglomerates. Figure 1 shows scanning electron micrographs of the powder before and after decomposition. They obviously confirm the agglomeration and also indicate that the decomposition does little to change the macroscopic shape or size of the particle. The agglomerate size distribution was also substantiated by measurements with a Coulter counter which indicated a very square distribution with greater than 95% in the size range of 20–60 μm.

Isothermal measurements

Samples were nominally controlled at 1, 2, 4, 8, 16, and 32 mgs. They were packed by light tapping into a small hemispherical basket of platinum having a radius of 2.5 mm. This basket was suspended in a fused quartz tube having an internal diameter of 18 mm. Oxygen was passed through a tower of Drierite and down the tube at a rate of approximately 60 cm^3 min^{-1}. The sample was then heated to constant weight at 400°C. A clam shell furnace at the desired temperature was then closed around the tube and data collection was begun. In this manner, the weight loss of each size sample was followed at 981, 952, 930, 910, and 880 K. The Cahn balance and the electronics, which obtain weight and temperature as a function of time in a digital format on magnetic tape, have been described elsewhere[2]. The subsequent computer processing has been previously described in some detail[2,3].

Figure 2 shows typical weight versus time plots from the first stage of computer analysis. The second stage involved fitting the data to a variety of kinetic rate laws. Table 1 lists the functions which were plotted versus time. The minimum standard deviation in alpha obtained from the least squares fitting of the best straight line was used as the criteria for the most applicable rate law. Some typical plots are shown

TABLE 1

KINETIC FUNCTIONS USED IN THE COMPUTER ANALYSIS (α = fraction reacted)

Power law	α^n, $n = 1, 2, \frac{1}{2}, \frac{1}{3}, \frac{1}{4}$
Contracting geometry	$1-(1-\alpha)^{1/n}$, $n = 2, 3$
Erofeev	$[-\ln(1-\alpha)]^{1/n}$ $n = 1, 1.5, 2, 3, 4$
Diffusion controlled, 2D	$(1-\alpha)\ln(1-\alpha)+\alpha$
Diffusion controlled, 3D	$(1-\frac{2}{3}\alpha)-(1-\alpha)^{\frac{2}{3}}$
Jander	$[1-(1-\alpha)^{\frac{1}{3}}]^2$
Prout–Tompkins	$\ln[\alpha/(1-\alpha)]$
Second order	$1/(1-\alpha)-1$
Exponential	$\ln\alpha$

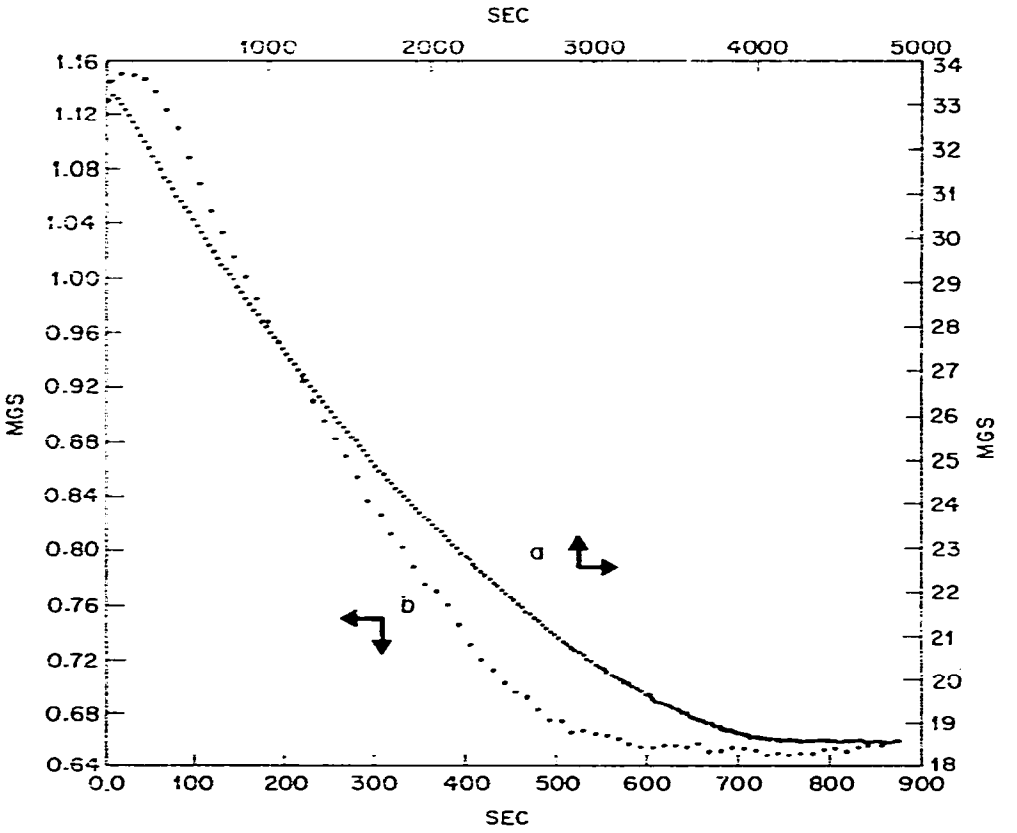

Fig. 2. Typical isothermal weight versus time plots, at 981 K.

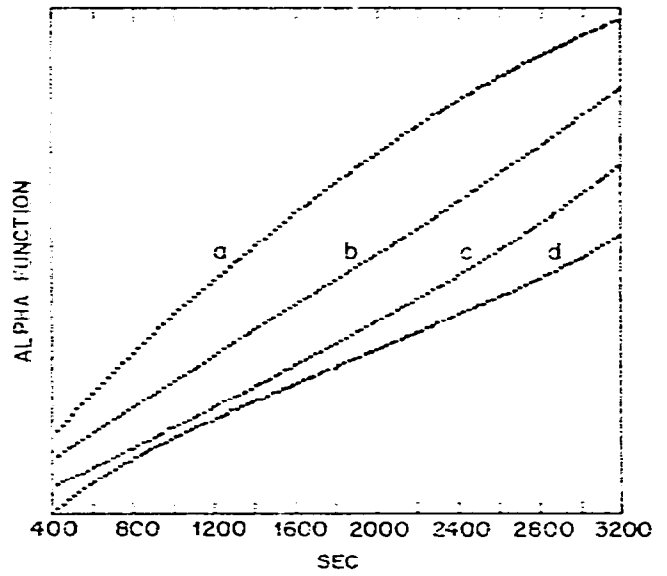

Fig. 3. Typical computer plots of alpha function versus time, 32 mg at 981 K. Alpha function: a, α; b, $1-(1-\alpha)^{\frac{1}{3}}$; c, $1-(1-\alpha)^{\frac{1}{2}}$; d, $[-\ln(1-\alpha)]^{\frac{1}{3}}$.

in Fig. 3. The least square line was determined over the range in alpha from 0.1 to 0.9 or approximately from 400 to 3200 sec in Fig. 3.

The contracting area equation

$$1-(1-\alpha)^{\frac{1}{2}} = kt \tag{1}$$

and the Erofeev equation with $n = 2$

$$[-\ln(1-\alpha)]^{\frac{1}{2}} = kt \tag{2}$$

were consistently the most applicable rate laws. Figure 4 uses the contracting area equation and indicates the resulting lines for varying sample weight at constant temperatures. Figure 5 presents similar data for varying temperature at constant sample weight.

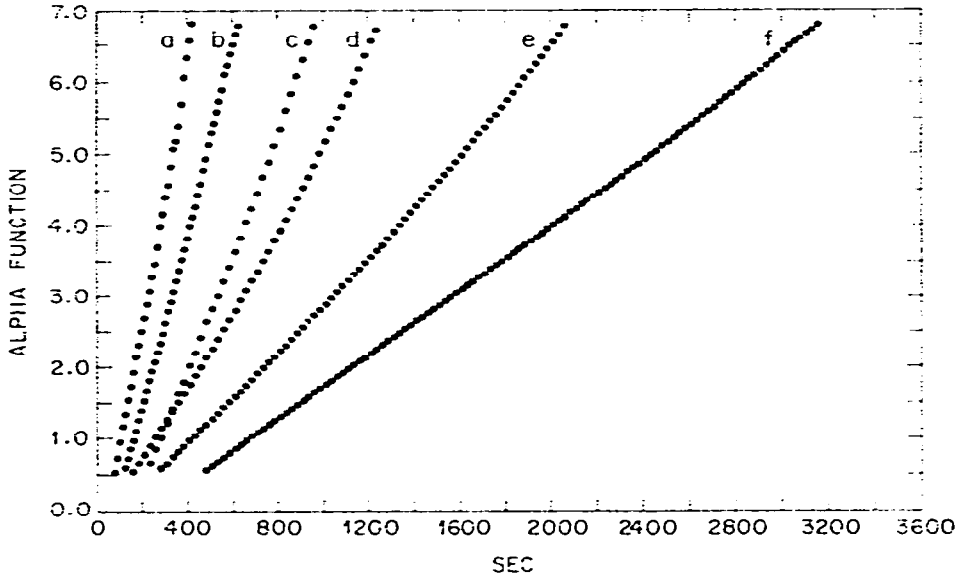

Fig. 4. Plots of $1-(1-\alpha)^{\frac{1}{2}}$ versus time at 981 K. a, 1.17 mg; b, 2.09 mg; c, 3.96 mg; d, 8.43 mg; e, 16.16 mg; f, 32.13 mg.

It was noted that plots of log k versus log weight (mg) were reasonable straight lines for each temperature. Figure 6 shows a typical plot with the least square lines. Such plots were used to correct the k's observed for the nominally correct weight to the exact weight increments of 1, 2, 4, 8, 16, and 32 mgs. These corrected k's were then combined with the Arrhenius equation to determine values of the activation enthalpy, ΔH^* and pre-exponential A, term for each sample weight. Figure 7 shows a typical Arrhenius plot. Derived values of ΔH^* were identical within ± 0.1 kcal using either rate law. The Erofeev equation consistently yielded a larger value of A.

Average values of ΔH^* and the separate values of log A were plotted versus log weight (mgs) in Fig. 8. Remarkably good straight lines result. The calculated

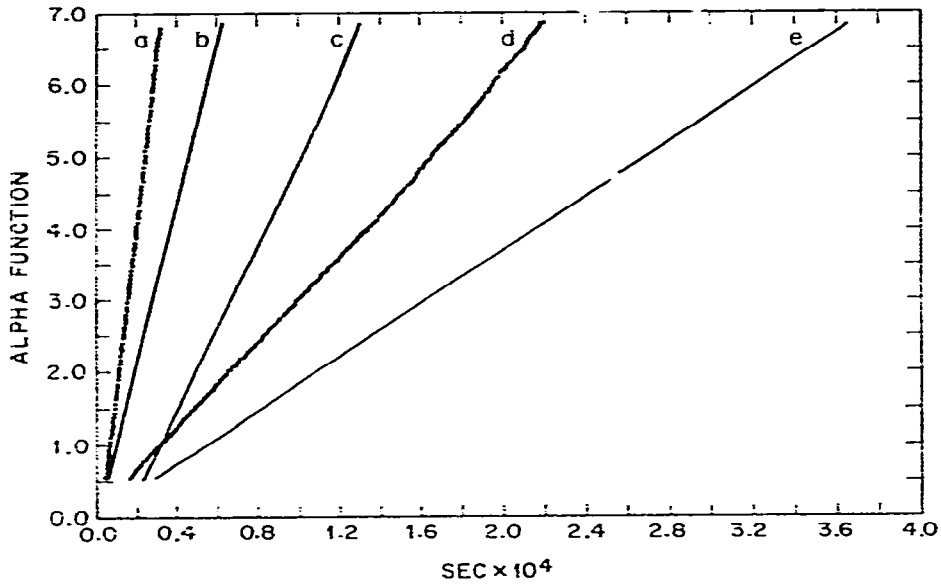

Fig. 5. Plots of $1-(1-\alpha)^{\frac{1}{3}}$ versus time for 32 mg sample. a, 981 K; b, 952 K; c, 930 K; d, 910 K; e, 880 K.

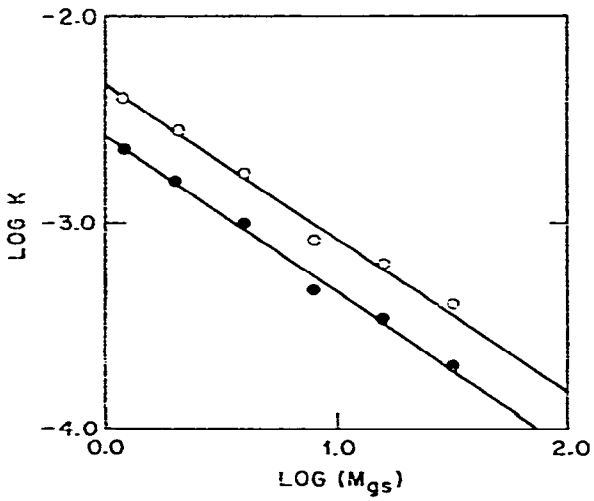

Fig. 6. Plot of log k versus log weight at 981 K. O, $1-(1-\alpha)^{\frac{1}{3}}=kt$; ●, $[-\ln(1-\alpha)]^{\frac{1}{3}}$.

equations from the least squares fit to the best straight lines are:

$$\Delta H^* \text{ (in kcal/mole)} = -2.9134 \log (\text{mgs}) + 49.675 \tag{3}$$

$$\log A_1 = -1.3152 \log (\text{mgs}) + 8.4026 \tag{4}$$

$$\log A_2 = -1.3425 \log (\text{mgs}) + 8.6597. \tag{5}$$

These equations fit all the points within $\pm 0.1\%$.

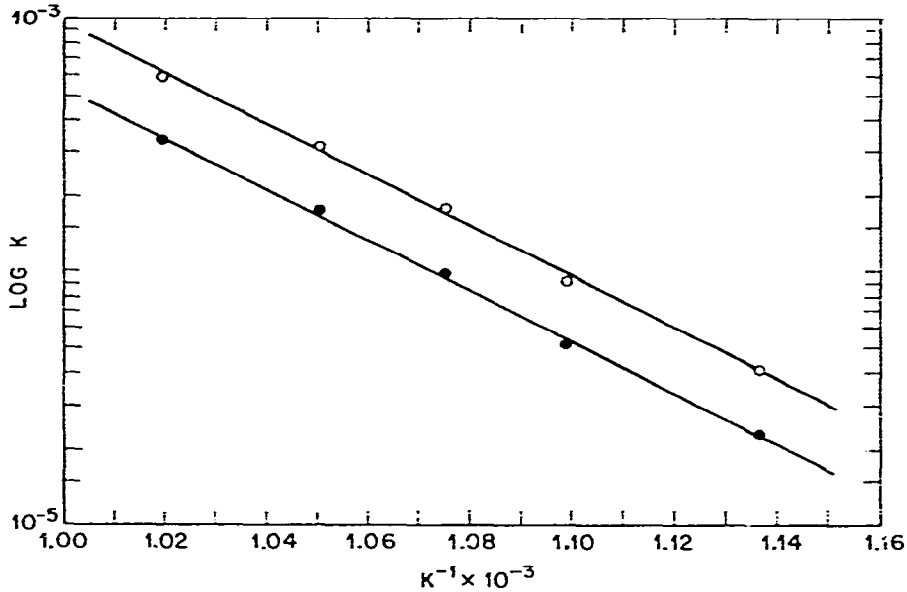

Fig. 7. Arrhenius plots for a 16 mg sample. O, $1-(1-\alpha)^{\frac{1}{3}} = kt$; ●, $[-\ln(1-\alpha)]^{\frac{1}{3}} = kt$.

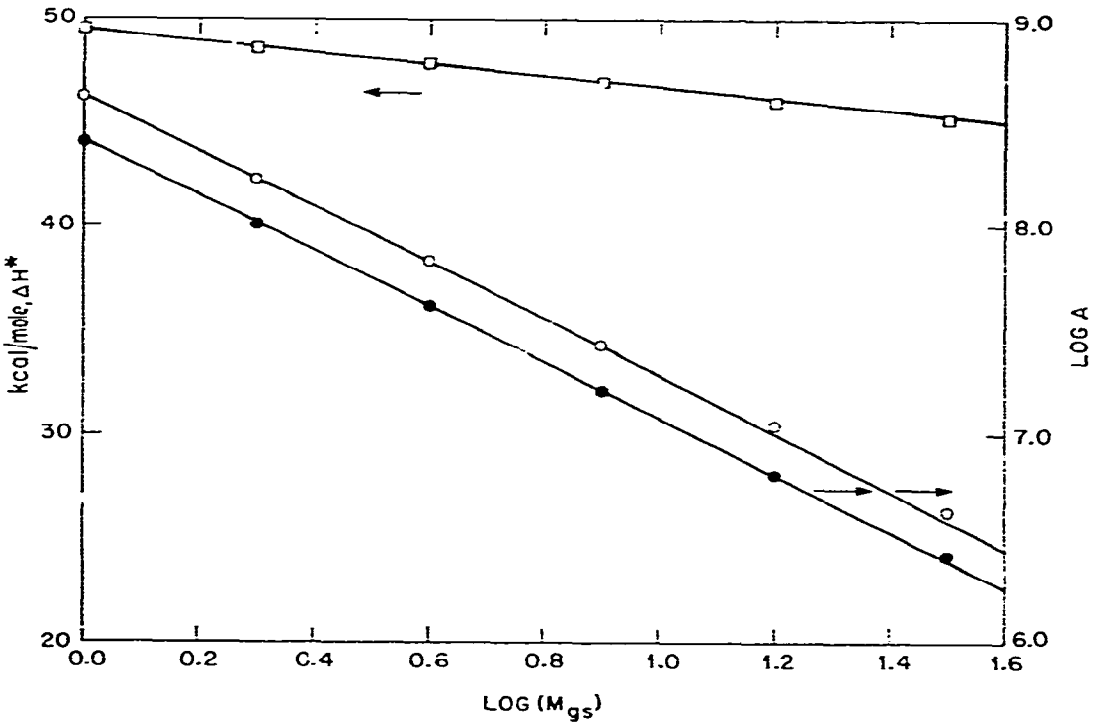

Fig. 8. Arrhenius parameters versus log weight (mgs) ΔH^*. O, log A for $1-(1-\alpha)^{\frac{1}{3}} = kt$; ●, log A for $[-\ln(1-\alpha)]^{\frac{1}{3}} = kt$.

Dynamic measurements

A Perkin–Elmer thermobalance was used. It had been modified to give a digital output on punched paper tape of weight and temperature as a function of time[4]. The temperature axis was calibrated using magnetic standards[4]. A flow of dry oxygen, 40 cm^3 min^{-1}, was maintained down the furnace tube, 20 mm i.d. The sample holder was a small cylindrical platinum cup about 3.5 mm in diameter and 1.2 mm deep. This limited the sample size to a maximum of 16 mg. Nominal sample weights of 1, 2, 4, 8, and 16 mgs were run at heating rates of 73.6, 18.2, 4.45, 1.16, and 0.29 C min. Figure 9 shows the resulting computer plots for the extremes in sample weight and heating rate. The 8 and 16 mg samples failed to go to completion at the fastest heating rate under the experimental conditions imposed.

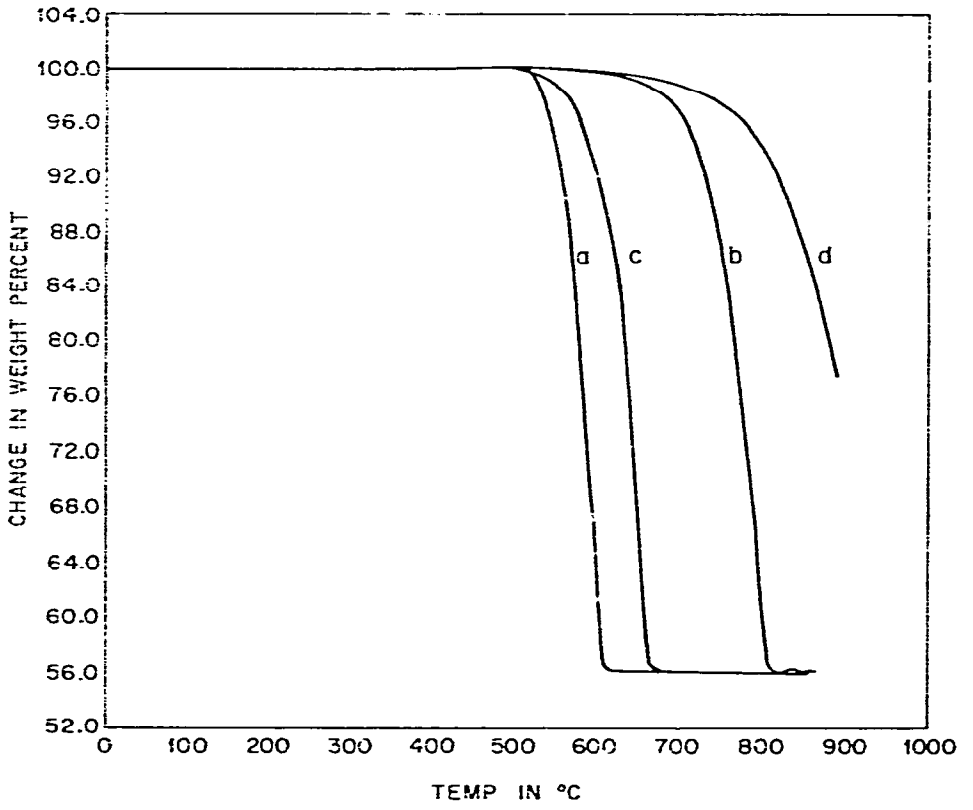

Fig. 9. Thermogravimetric plots for a, 1.25 mg at 0.29 C min; b, 0.95 mg at 73.6 C min; c, 15.86 mg at 0.29 C min; d, 16.05 mg at 73.6 C min.

These data were processed to give values of ΔH^* and A using three basic techniques[5]. The Freeman and Carroll[6] approach is a difference-differential technique in which the order of the reaction is determined as well as the Arrhenius parameters. An integral technique was developed by Coats and Redfern[7]. The Achar, Brindley, and Sharp[8] method is a single differential method. The last two methods require the order of the reaction as an input. Values of 0, 0.5, 0.67, and 1.0 were used but the

standard deviations obtained using 0.5 were generally the lowest. This order corresponds to the contracting area equation, eqn (1), described earlier. Table 2 summarizes the results.

TABLE 2

SUMMARY OF THE DYNAMIC STUDIES ON THE THERMAL DECOMPOSITION OF $CaCO_3$ IN DRY OXYGEN

Temp. rate °C/min	*Weight* mgs.	*ABS*[a]		*CR*[b]		*FC*[c]		*n*[e]
		ΔH^*[d]	*log A*	ΔH^*[d]	*log A*	ΔH^*[d]	*log A*	
73.6	1.25	53.4	9.08	55.5	9.54	58.4	10.04	0.63
	2.08	50.9	8.36	54.5	9.11	52.6	8.66	0.56
	4.07	44.2	6.58	48.3	7.42	47.5	7.18	0.61
	8.73	45.7	6.65	45.5	6.62	45.7	6.66	0.47
	16.05	44.2	6.11	37.5	4.81	45.0	6.26	0.52
18.2	0.77	56.6	10.18	61.6	11.30	59.9	10.83	0.58
	2.15	55.0	9.36	55.9	9.53	44.3	7.11	0.21
	4.39	51.2	8.20	51.4	8.23	48.5	7.65	0.40
	7.79	50.8	7.89	48.6	7.43	52.4	8.15	0.58
	16.72	45.7	6.54	42.7	5.92	47.4	6.84	9.55
4.45	0.94	60.5	11.32	66.5	12.75	70.6	13.42	0.79
	2.30	59.3	10.59	61.5	11.11	52.8	9.15	0.35
	4.20	59.0	10.28	58.1	10.04	50.1	8.32	0.25
	8.14	54.8	8.99	55.1	9.04	50.4	8.04	0.38
	16.16	52.5	8.20	50.8	7.82	47.6	7.18	0.38
1.16	1.09	63.4	11.80	62.0	11.46	62.5	11.58	0.48
	2.22	60.5	10.81	60.2	10.73	46.9	7.69	0.14
	3.81	58.3	10.04	56.8	9.66	53.4	8.95	0.38
	8.18	61.9	10.53	56.3	9.20	58.6	9.76	0.46
	16.24	56.1	9.04	52.3	8.18	44.5	6.51	0.17
0.29	0.96	54.8	9.74	55.4	9.89	34.3	4.69	−0.18
	2.11	60.2	10.82	56.9	10.00	67.3	12.45	0.69
	3.76	59.4	10.45	55.6	9.46	55.2	9.45	0.42
	7.81	55.3	10.04	51.4	9.08	42.5	7.00	0.11
	15.86	56.7	9.36	51.5	8.11	46.0	7.88	0.18

[a]Differential method of Achar, Brindley and Sharp[8]. $n = 0.5$. [b]Integrating method of Coats and Redfern[7]. $n = 0.5$. [c]Difference-differential method of Freeman and Carroll[6]. [d]in kcal/mole. [e]n = order of reaction.

Berlin and Robinson[9] have described a technique whereby ΔH^* can be obtained from the slope of the line formed from a plot of log (K/sec) versus T_f^{-1} where T_f is the absolute temperature at which the weight loss stops. Figure 10 shows such plots for those thermogravimetric experiments which went to completion. The points do not form a straight line. Using the values at the slower heating rates, which are more linear, values of ΔH^* from 44 to 37 kcal/mole are calculated. The values decrease with increasing weight.

Berling and Robinson[9], using the data of Richer and Vallet[10], observed a straight line relationship between log (mgs) and T_f^{-1}. Figure 11 shows such plots for this work.

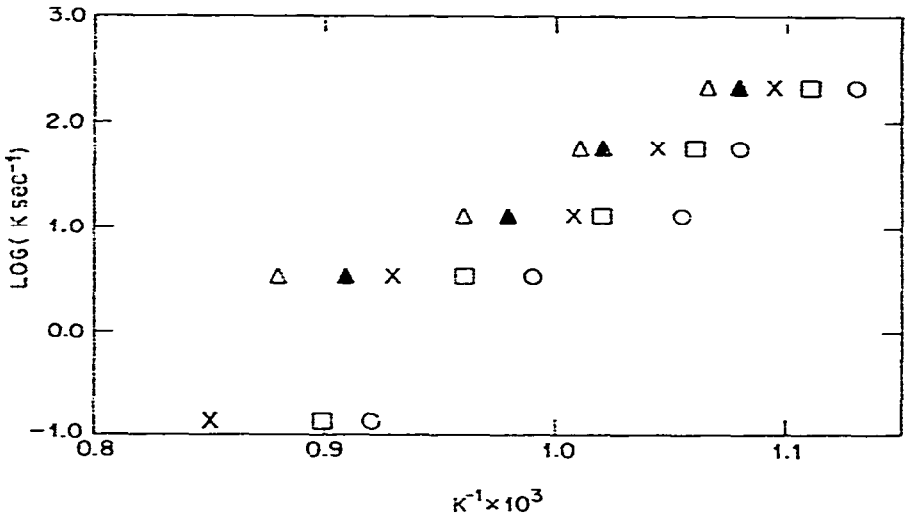

Fig. 10. Plots of log (K sec^{-1}) versus the reciprical of the temperature of complete decomposition. O, 1 mg; ×, 2 mg; □, 4 mg; ▽, 8 mg; ▼, 16 mg.

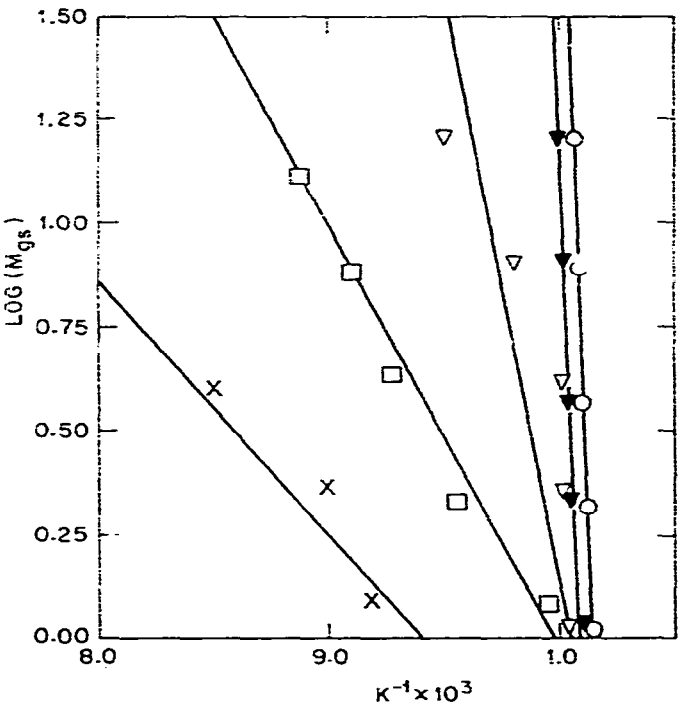

Fig. 11. Plots of log (mgs) versus the reciprical of the temperature of complete decomposition; ×, 73.6 K/min; □, 18.2 K/min; ▽, 4.45 K/min; ▼, 1.16 K/min; O, 0.29 K/min.

DISCUSSION

The discussion of the isothermal results will be restricted to the contracting geometry rate law. Although the Erofeev equation with $n = 2$ fits equally well, the contracting geometry is conceptually simpler and has the added advantage of being more compatible with the dynamic techniques[5]. As in prior work[2,3,5] the value of ΔH^* was relatively independent of the choice of rate law. Only the values of A varied significantly.

Equations (3) and (4) can be substituted into the Arrhenius equation to yield

$$\log k = (636.7\ T^{-1} - 1.3152) \log (\text{mgs}) + 8.4026 - 10\,855\ T^{-1}. \quad (6)$$

This equation describes the experimentally observed rate constant as a function of sample weight and temperature. Figure 12 shows plots of log K versus T^{-1} for a large range of sample weights. Besides 1 and 32 mgs, which represent the extremes of this

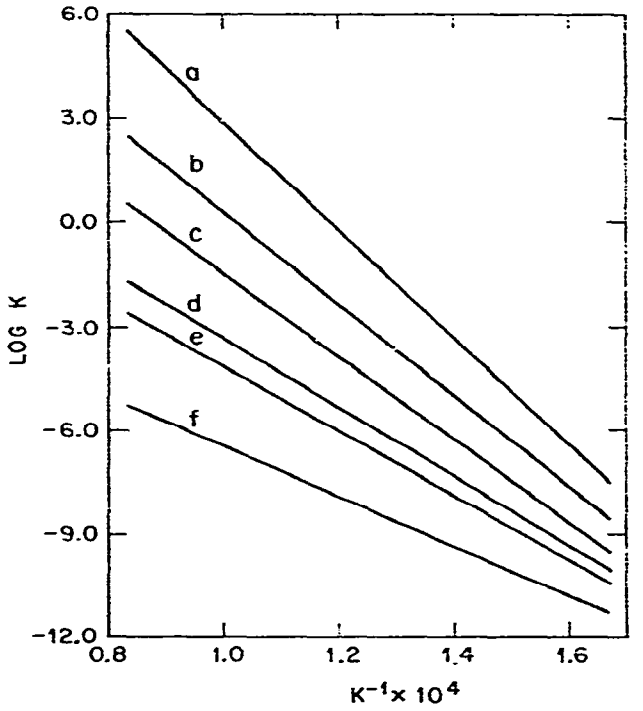

Fig. 12. Arrhenius plots as a function of sample weight: a, 1.135×10^{-8} mg; b, 6.62×10^{-5} mg; c, 1 mg; d, 32 mg; e, 500 mg; f, 10^6 mg.

investigation, there are lines for a hypothetical 36 μm and 1 μm particles representing a single experimental aggregate and particle respectively. At the other extreme there are lines representing a more conventional sample weight of 500 mgs and finally a kilogram.

Although log k can be accurately expressed in terms of sample weight, the extrapolation to zero weight leads to an infinite value of the rate constant. Similarly extrapolations for ΔH^* and log A to zero sample size also give values of infinity. The contracting geometry model assumes instant surface nucleation and then a constant, zero order, rate of movement of the interface inward. The experimentally determined rate constant is the true zero order rate constant for interface movement divided by the appropriate geometric parameter *e.g.*, radius of the spherical particle, one half of the edge for a cubic particle, or radius of the circular cross section for a cylindrical particle reacting in two dimensions. Consequently as the sample weight and thus size goes to zero the experimental rate constant will go to infinity. However, the model assumes rapid surface nucleation, and therefore is no longer applicable for data taken from very small particles where the surface molecules represent a significant fraction of the total.

Because the samples were sized the radius of the aggregates are presumably the same and thus the experimental rate constants should all be different from the true zero order rate constant by a constant amount. However, Ingraham and coworkers[11,12] have shown that pelletized samples can behave essentially as a single, large particle with the reaction interface proceeding inward. Although the samples in this work were not pelletized it is nevertheless reasonable that the bulk pile geometry would be a factor. The reasons for localized CO_2 concentrations and thermal transport are still valid. In order to determine the appropriate conversion factor it is necessary to establish the shape of the bulk sample. Pelletizing as advocated by Ingraham and coworkers[11,12] would seem to solve this; however, with the small sample weights used herein this was not considered feasible. Even once this is established there is still the tacit assumptions that the geometrical shape remains constant and that all surfaces receive the same thermal flux. It is basically a combination of the pile geometry and the distribution of thermal flux that determines the apparent order of the reaction.

Since this connection represents a constant multiplier of the rate constant it is not a factor in the determination of ΔH^* when a constant sample size is employed. In other words, there is no change in eqn (3). The difference appears as a correction to the pre-exponential term. If for example, the sample was assumed to be a spherical pile behaving as a single particle then eqn (6) becomes

$$\log k_{true} = (636.7\, T^{-1} - 0.9819) \log (\text{mgs}) + 9.9520 - 10\,855\, T^{-1} \qquad (7)$$

The true rate constant, or rate of interface motion, would also have units of μm sec^{-1} where the radius of the sample pile is in μm. Such a correction does reduce the dependence of the rate constant on sample weight but it can never eliminate it because of eqn (3). New lines for each weight such as those shown in Fig. 12 would be parallel to the old but the spread would be significantly less.

The second major factor in introducing a dependence of k, ΔH^*, and A upon sample weight is the effect of self cooling in an endothermic process. The ΔH^* involved in this and most other decomposition reactions is immense in comparison

to the heat capacity of the products and reactants. Under hypothetical adiabatic conditions it would be sufficient to lower the sample temperature over a thousand degrees. Obviously, therefore, it is necessary to have a high thermal input in order to sustain the reaction. This heat must be supplied from conduction by the sample holder and atmosphere or by a radiant flux and in either case must diffuse through the product layer of increasing thickness to the reaction interface. As described in the introduction this thermal exchange is favored by small sample size and slow decomposition rates.

Equation 7 offers some indication of the extent of self cooling. Table 3 gives values of temperature calculated at different reaction rates for the sample weights used in Fig. 12. These temperatures correspond to the experimental temperature as

TABLE 3

EXPERIMENTAL[a] REACTION TEMPERATURES FOR VARIOUS REACTION RATES AND SAMPLE WEIGHTS

Weight (*mg*)	k_{true} ($\mu m\ sec^{-1}$)		
	10^{-4}	10^{-2}	1
1.135×10^{-8}	732 K	806 K	896 K
6.62×10^{-5}	749	842	962
1	778	908	1091
32	793	945	1168
500	808	982	1251
10^{6}	873	1161	1732

[a]Calculated from eqn. (7).

measured in this work. If one assumes that the temperature indicated for the 1 μm particle is very nearly correct, then in the region where this work was done, *i.e.*, $k_{true} \approx 10^{-2}$, the measured thermocouple temperature was approximately 100–140° higher than the actual interface temperature. This degree of self cooling is similar to that determined by Draper and Sveum[13]. The advantages of working at the lower temperatures and the slower reaction rates is also substantiated by Table 3. As the rates become slower, the temperature discrepancy becomes smaller.

Another possible reason for the dependence of the Arrhenius parameters upon sample weight is the relative change in the partial pressure of CO_2. The larger the sample size, the longer the diffusion path of the CO_2 and hence the greater the partial pressure of CO_2. The equilibrium constant would then require a higher reaction temperature for the larger samples. However, it is assumed that the diffusion of the gaseous products out of a lightly taped powdered sample is substantially greater than the diffusion of heat in and is therefore a minor factor. This is substantiated by the fact that Britton *et al.*[14] obtain values of ΔH^* in vacuum which are comparable to most of the values determined in a sweep gas[11].

If there is no significant change in the partial pressure of CO_2 then thermodynamics would predict that the reaction temperature is where $\Delta G = 0$, at the appropriate partial pressure of CO_2. Provided that $\Delta H^* = \Delta H$, the reaction would proceed at a measurable rate[13]. However, this stipulation that the solid state reaction proceeds without activation appears unlikely. The thermodynamic enthalpy of the reaction is defined for the products in their standard state. At the very least the CaO initially formed by the decomposition is in a microcrystalline or amorphous and highly strained state with a large concentration of defects. This regardless of any additional mechanistic difficulties should give rise to $\Delta H^* > \Delta H$ on a microscopic scale. The time, temperature, and particle size relationships may be such that this additional energy is retrieved on a macroscopic scale before the rate measurements are concluded. Under those circumstances ΔH^* could approach ΔH. It is the contention of this paper therefore that the reaction temperature is probably not independent of sample size, particularly for the smaller sample sizes.

The results of the dynamic experiments suggest that they lack the precision or consistency of the isothermal results. Table II reveals considerable scatter in the values of ΔH^* among the various experimental situations, and even more distressing among the various methods of analysis for the same data. They do indicate, however, that a single simple experiment can give a reasonable estimate of the Arrhenius parameters with careful analysis. Alternatively the very simple analysis suggested by Berlin and Robinson[9] combined with several experiments can give a suitable estimate of ΔH^*. Figure 10, however, indicates that the proposed relationship is not linear over a very wide range of heating rates. The Berlin–Robinson approach did predict a $(\text{mgs})^{\frac{1}{3}}$ dependence[9] which is in excellent agreement with eqn (3). Although in eqn (3) the dependence of ΔH^* upon weight has a temperature term, the average value is very nearly $\frac{1}{3}$ over the experimental range of temperature.

As expected the scatter and lack of smooth trends is most evident in the Freeman–Carroll technique[5]. This is in a large part due to the added degree of freedom afforded by the selection of the order, n. The value of n varies considerably but the average is 0.4. In both the Coats–Redfern[7] and the Achar, Brindley and Sharp[8] analysis as well as in the isothermal treatment, the values of n were restricted to 0, 0.5, 0.67, and 1.0. The value of 0.5 gave consistently the best results so that all the data and analytical approaches are consistent in this respect.

Certain trends are clearly evident from the dynamic results. The values of ΔH^* and A tend to increase with decreasing sample weight and heating rate. Qualitatively these trends are in complete agreement with conclusions based upon isothermal results. Reducing the heating rate slows the reaction and provides for better thermal equilibrium.

Table 4 offers a comparison of the results of this work with some previous investigations. In general, the other investigations employed sample sizes much greater than used herein. Equation (3) predicts that $\Delta H^* = 41.8$ kcal/mole for a sample weight of 500 mg. This is in good agreement with the previous values. There does not appear to be any consistent difference between the values based on either dynamic

TABLE 4
SOME EXPERIMENTAL VALUES FOR THE THERMAL DECOMPOSITION OF $CaCO_3$

Investigators	ΔH^* (*kcal/mole*)	*Sample wt* (*mg*)	*Dynamic isothermal*	*Atmosphere*	*Order*
Berlin and Robinson[9]	40.6	250	D	N_2	—
Britton, Gregg and Windsor[14]	35–42	500	I	vacuum	0.58–0.72
Coats and Redfern[7]	51.7	100	D	air	0.46
Draper and Sveum[13]	41.2	300–450	I	N_2	—
Freeman and Carroll[6]	39.0	290	D	air	0.4
Hutlig and Kappal[15]	49	—	I	—	0–1
Ingraham and Marier[11]	40.6	455	I	air	0.67
Kissinger[16]	42.9	—	I	—	0.22
Maskill and Turner[17]	95	500–2000	I	air	1
Slonium[18]	38.0	—	I	vacuum	1
Speros and Woodhouse[19]	44	100	D	N_2	0.2
Sharp and Wentworth[20]	43–46	1000	D	—	0.5
Splichel *et al.*[21]	37–39	—	I	—	0.3
This work	49.7–45.3	1–32	I	O_2	0.5
This work	34–71	1–16	D	O_2	~0.5
This work extrapolated	41.8	500	I	O_2	0.5

or isothermal techniques. The order shows considerable variation but it must be recalled that both the sample geometry and the distribution of thermal flux are involved. A spherical sample which is heated primarily on the sides adjacent to the furnace walls cannot be expected to follow a simple contracting sphere rate law.

SUMMARY AND CONCLUSIONS

Although the dependence of the rate constant, activation enthalpy, and pre-exponential term upon sample weight is not new[8,17,22], it was carefully determined over a wide range and with smaller samples than previously employed. Extrapolation to higher weights give values which are consistent with previous investigations. Unfortunately, the logarithmic dependence upon weight precludes extrapolation to zero weight.

The dependence of the Arrhenius parameters upon weight is a composite of at least four factors. Since the data best fit the contracting geometry equation with $n = 2$, it must be remembered that this model will break down when a significant portion of the total reactant molecules are present in the surface. This, however, should not become a factor until the particle size approaches 100 Å. The actual value of n depends upon the distribution of thermal flux as well as sample geometry.

The second factor concerns the geometry of the sample pile and its tendency to behave as a large single particle. The experimental rate constant represents the true zero order rate constant for the interface motion divided by a particular geometric

distance depending upon assumed geometry of the sample. Individual particle size also is a factor but to a lesser degree[11].

The self cooling effect of an endothermic reaction is an established fact and it plays a dominant role. The larger the sample size the greater the difficulty of equilibrating with the experimental heat sink of finite capacity, *i.e.*, the sample holder. The length of the thermal diffusion path also becomes greater depending upon the extent of the reaction and hence larger temperature differentials become possible. This is strongly dependent upon the rate of the reaction and can be greatly minimized by working at lower temperatures or heating rates.

The partial pressure of CO_2 will govern the equilibrium decomposition temperature. The larger the sample the longer the diffusion path. Consequently, the partial pressure is more likely to build up and raise the equilibrium decomposition temperature. This is considered to be a minor effect compared to the thermal diffusion and bulk sample geometry.

This composite view implies that the actual ΔH^* of the reaction is significantly larger than the values generally measured. At the lightest sample actually measured, about 1 mg, ΔH^* is 49.7 kcal/mole. The problem remains regarding how far it is valid to extrapolate. Extrapolation to the slightly higher weights used in other investigations, see Table 4, appears successful. If the extrapolation is carried to a single 1 μm spherical particle, the smallest entity of the experimental samples, or to a 100 Å particle, an approximate lower limit of the contracting geometry model of the rate law, then the values of ΔH^* become 72.5 and 90.3 kcal/mole respectively. These values agree well with the intrinsic values proposed for the threshold of the decomposition of carbonate ions[9,17,23].

ACKNOWLEDGMENT

The authors are grateful to Mr. H. Leamy for the scanning electron micrographs and to Mr. F. Schrey for measurement of the surface area.

REFERENCES

1 K. H. Stern and E. L. Weise, *High Temperature Properties and Decomposition of Inorganic Salts*, Part 2, *Carbonates*, NSRDS-NBS 30, No. 1969, U. S. Government Printing Office, Washington, D.C.
2 P. K. Gallagher and D. W. Johnson Jr., *Thermochim. Acta*, 4 (1972) 283.
3 D. W. Johnson Jr. and P. K. Gallagher, *J. Phys. Chem.*, 75 (1971) 1179.
4 P. K. Gallagher and F. Schrey, *Thermochim. Acta*, 1 (1970) 465.
5 D. W. Johnson Jr. and P. K. Gallagher, *J. Phys. Chem.*, 76 (1972) 1474.
6 E. S. Freeman and B. Carroll, *J. Phys. Chem.*, 62 (1958) 394.
7 A. W. Coats and J. P. Redfern, *Nature*, 201 (1964) 68.
8 B. N. N. Achar, G. W. Brindley and J. H. Sharp, *Proc. Int. Clay Conf., Jerusalem*, 1 (1966) 67.
9 A. Berlin and R. J. Robinson, *Anal. Chim. Acta*, 27 (1962) 50.
10 A. Richer and P. Vallet, *Bull. Soc. Chim Fr.*, (1953) 148.
11 T. R. Ingraham and P. Marier, *Can. J. Chem. Eng.*, 41 (1968) 170.
12 N. A. Warner and T. R. Ingraham, *Can. J. Chem. Eng.*, 40 (1962) 263.
13 A. L. Draper and L. K. Sveum, *Thermochim. Acta*, 1 (1970) 345.

14 H. T. S. Britton, S. J. Gregg and G. W. Windsor, *Trans. Faraday Soc.*, 48 (1952) 63.
15 G. F. Huttig and H. Kappal, *Angew. Chem.*, 53 (1940) 57.
16 H. E. Kissinger, *Anal. Chem.*, 29 (1957) 1702.
17 W. Maskill and W. E. S. Turner, *J. Soc. Glass Technol.*, 16 (1932) 80.
18 G. Slonium, *Z. Electrochem.*, 36 (1930) 439.
19 D. M. Speros and R. L. Woodhouse, *J. Phys. Chem.*, 72 (1968) 2846.
20 J. H. Sharp and S. A. Wentworth, *Anal. Chem.*, 41 (1969) 2060.
21 J. Splichel, St. Skromovsky and J. Goll, *Collect. Czech. Chem. Commun.*, 9 (1937) 302.
22 P. Murray and J. White, *Trans. Brit. Ceram. Soc.*, 54 (1955) 189.
23 B. Bruzs, *J. Phys. Chem.*, 30 (1926) 680.